Available online at www.sciencedirect.com
SCIENCE DIRECT®
Computers and Structures 83 (2005) 895–908
Computers & Structures
www.elsevier.com/locate/compstruc

A model for hysteretic behavior of rhombic low yield strength steel added damping and stiffness

Ming-Hsiang Shih [a], Wen-Pei Sung [b,*]

[a] Department of Construction Engineering, National Kaoshiang First University of Science and Technology, Kaoshiang 811, Taiwan, ROC
[b] Department of Landscape Design and Management, National Chin-Yi Institute of Technology, Taichung 41111, Taiwan, ROC

Received 24 April 2004; accepted 23 November 2004
Available online 20 January 2005

Abstract

The Low Yield Strength Steel (LYS) has the superiority over long period of low cycle fatigue, high strain hardening rate and impressive ductility to overcome the local fracture problem existing in regular A36 steel plate. With elastoplastic characteristics and experimental verification, it becomes a good material considered for added damping and stiffness (ADAS) since the stress–strain relationship of LYS performs yielding much earlier than that of A36 steel. Thus, Wen's Model and the bi-linear model, simulated for A36 energy absorber cannot properly analyze energy dissipation while A36 are replaced by LYS. Therefore, the modified Wen's Model is proposed to reproduce the complicated nonlinear strain hardening in seismic resistance of rhombic LYS under reciprocating loading test. The numerical simulation and experimental data can match each other to reveal that the proposed model has capability in predicting the hysteresis energy dissipation behavior of rhombic low yield strength steel plate. This model also can be easily integrated with a dynamic analysis program.

Keywords: Modified Wen's model; Hysteresis energy dissipation behavior; Seismic resistance of LYS; Dynamic analysis; Pseudo-dynamic tests

1. Introduction

X [1,2] and triangular [3,4] type of steel plates both are most often selected for the earthquake resistant device of adding damping and stiffness (ADAS). Nevertheless, axial force and welded bond still influence these two types of devices. Meanwhile, it is hard to describe the force–deformation behavior of ADAS, especially when the strain hardening is occurred within nonlinear region of stress–strain diagram. Sozen [5] proposed that the hysteretic behavior of structure must be considered in the analysis model to expound the significant damping capability. To predict the hysteretic behavior of ADAS precisely, Tsai's team [2] suggested the elastic–perfectly plastic and elastic–linear work-hardening model to portray these phenomena. In order to enhance the energy dissipation capability of metallic damper, a new type of steel with low yield strength has been developed by China Steel Corporation Company. The investigation for this material shows that the ratio of the ultimate elongation is about 62% [6], yielding strength of LYS is below two thirds yielding strength of often-used steel

* Corresponding author.
E-mail address: sung809@chinyi.ncit.edu.tw (W.-P. Sung).

0045-7949/$ - see front matter © 2004 Elsevier Ltd. All rights reserved.
doi:10.1016/j.compstruc.2004.11.012

A36 and Low cycle fatigue of LYS is 4.5 times that of A36 steel [7]. The tested results revealed that higher yielding strength of LYS resulted in lower low cycle fatigue. By reviewing formal research, an innovative device—rhombic plate with Low Yield Strength Steel (LYS)—is integrated with ADAS for seismic resistance based on the consideration of structure, implementation and material property to improve the defects existing in traditional dampers. Figs. 1 and 2 show the configuration and installation of the proposed device. Photos 1–3 show the proposed device in test. These modifications are expected to reach the following advantages:

1. The rhombic steel plate has the characteristics in structural symmetry that can induce the reaction of fixed end moment of triangular-ADAS at the center of the rhombic steel plate. It helps manufacturers get rid of unqualified welded bond and save the cost.
2. The roller-supported connection at the both ends of rhombic steel plate can eliminate transfer axial force.
3. The curvature transformation of force–strain relationship at any point of rhombic steel plate, from Fig. 3, is almost same while dissipating energy. It means that the plate can yield uniformly and the problem of local fracture at the steel plate of energy dissipater can be overcome.

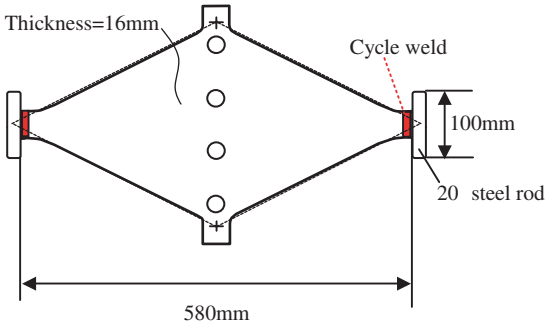

Fig. 1. The rhombic steel plate for ADAS.

The results of seismic test in Fig. 4 illustrate that the device with LYS displays perfect energy dissipation capability while Fig. 5 implies the ductility of LYS is 2–3 times larger than that of the A36 steel.

In order to analyze the energy dissipation behavior of the proposed device, a reliable simulation model is generated for more complicated material variables. According to the investigations for LYS material, the seismic resistance capability tests indicate that the stress–strain curve of LYS is quite different from that of A36 steel because LYS has no obvious yield stress plateau. Preceding the previous research with the concept of plasticity, Tsai and Chou [8] further proposed one-dimensional fiber model to explain the isotropic hardening of LYS. The Wen's Model [9,10] is well known as one of the best simulation tools for nonlinear analysis. However, this model is improper to reflect the isotropic hardening characteristics of LYS-ADAS. Fig. 5 shows the performance discrepancy of ADAS installed by LYS and A36 steel applied on ADAS. It implies the isotropic hardening of LYS is more apparent than that of A36 so that Wen's bi-linear model will lack sufficient parameters to describe the behavior of LYS-ADAS. Bouc–Wen Model [9,11,12] revised original Wen's model to discuss stiffness and strength degradation but excluded isotropic hardening. Barber and Wen [13] multiplied a weight variable, which is decreasing by yielding displacement, to reduce hardening rate as well as modify the parameter related to the yielding displacement to satisfy the maximum displacement. Zhang et al. [14] used the concept of Barber and Wen method to extend Bouc–

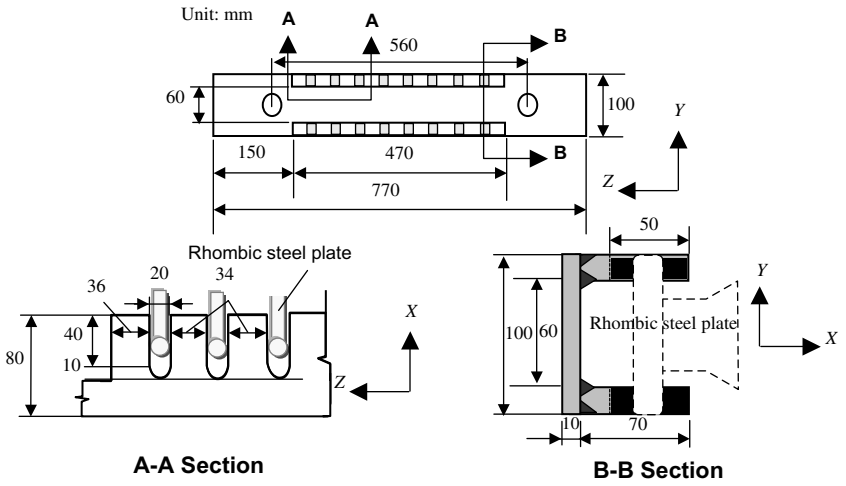

Fig. 2. The slot type bearing support of this newly developed seismic device.

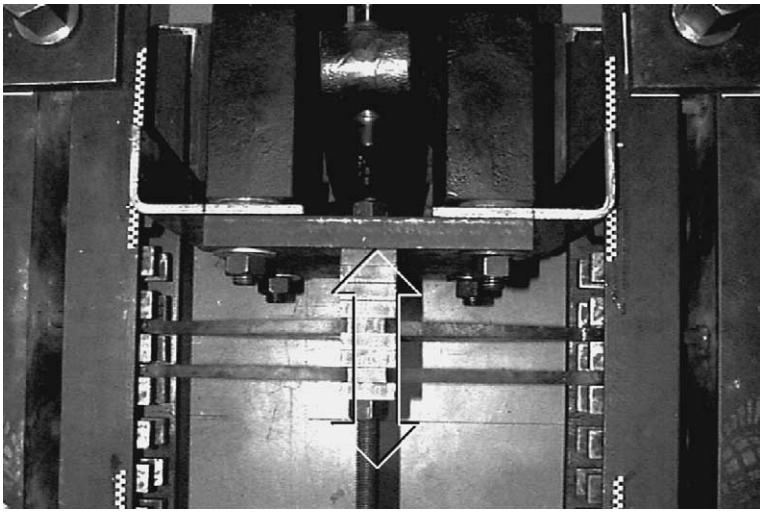

Photo 1. Top view of rhombic ADAS in test with actuator and loading direction.

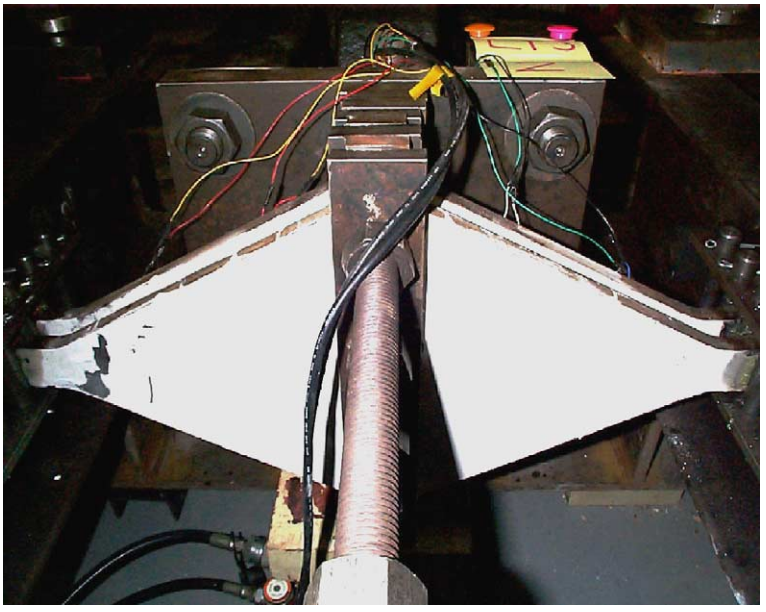

Photo 2. Side view of rhombic ADAS in test with actuator and loading.

Wen hysteretic model for estimating the simplex, extended Kalman filter and generalized reduce gradient methods.

Herein, the proposed model refers Barber and Wen's concept and alters the equation of Wen's model by differentiating and discretizing the transformation displacement variable to carry out the increment of restoring force as linear function of three displacement variables. Then, the optimal parameter can be recursive with the least square method. This algorithm considers the error between real material and numerical simulation while the noise signal cannot be completely neglected in the test so that the energy dissipation of new metallic damper can be practically demonstrated.

2. Theoretical model

2.1. An overview of Wen's Model

With essential parameters, Wen's Model can efficiently process nonlinear simulation, especially the

Photo 3. Detailed combination of rhombic ADAS.

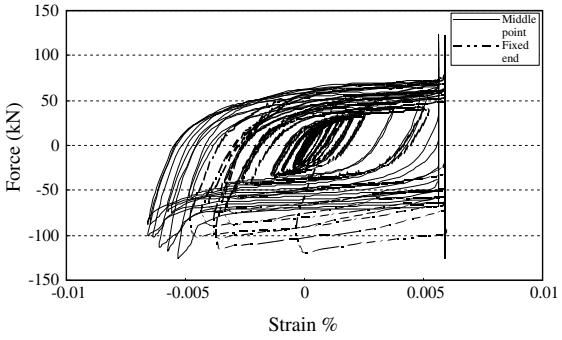

Fig. 3. The curvature transformation of rhombic steel plate.

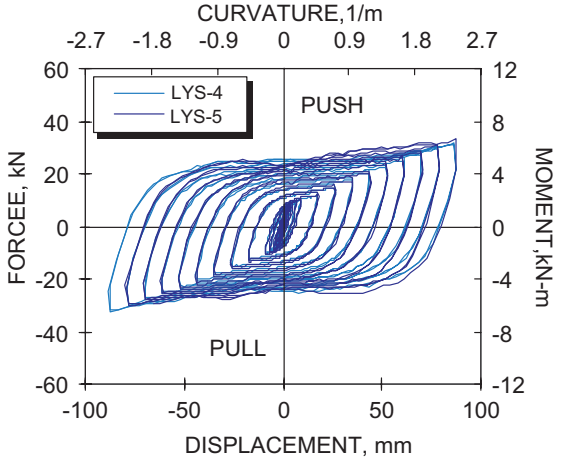

Fig. 4. The hysteresis energy dissipation behavior of newly developed seismic device.

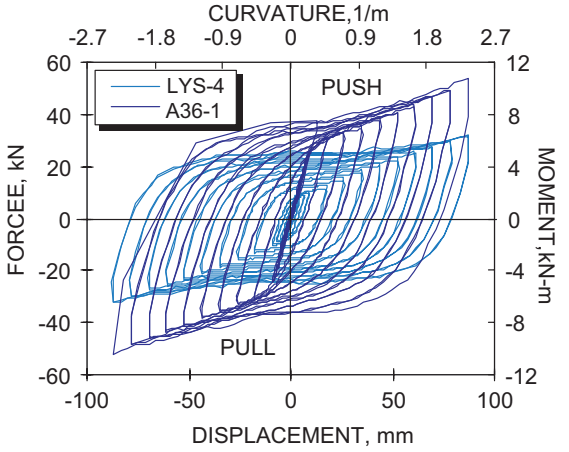

Fig. 5. The comparison of hysteresis dissipation behavior of LYS and A36.

hysteresis behavior that performs the loop by smooth and tender curve. The relationship of hysteresis restoring force $R(t)$ and displacement x defined in Wen's Model is

$$R(t) = \upsilon K_0 x + (1-\upsilon)K_0 q \tag{1}$$

$$\dot{q} = \alpha\dot{x} - \beta|\dot{x}||q|^{n-1}q - \gamma\dot{x}|q|^n \tag{2}$$

where x is the system displacement; $R(t)$, hysteresis restoring force; K_0, system initial stiffness; υ, stiffness rate before and after yielding; q, transformed displacement variable; α, β, γ and n, parameters to control the transformed hysteresis loop.

Eqs. (1) and (2), α, β, γ and n explains following two properties:

(1) The range of q, the maximum elastic displacement, is restricted by the equation:

$$|q| \leqslant \left(\frac{\alpha}{\beta+\gamma}\right)^{1/n} \tag{3}$$

(2) q is stable as $n \geqslant 1.0$. n has the effect in the radius of curvature. The larger n leads perfectly elastoplastic hysteresis loop while the smaller n means the curve of loop is going smoothly and gently. Therefore, Sues et al. [10] suggests that the n should be set as 1.0.

In general, Wen's Model is familiar with the nonlinear behavior of regular steel. Sues et al. [10] proposed modified parameter identification for the model based on the least square formulation to recognize the intensity and stiffness degrading behavior of members. However, Wen's Model is unsuitable for analyzing the strain hardening of low yield strength steel.

2.2. Hardening rule

A successful seismic resistance model must be able to reflect the hardening characteristic of steel and energy dissipation performance, so that the nonlinear phenomena of steel under reciprocating loading test can be behaved easily and accurately. As follows denotes the rules regarding isotropic hardening, kinematic hardening and hybrid hardening:

1. *Isotropic hardening rule*: Before the force is restituting, the yield stress is equal to the maximum stress acted by loading in opposite direction. It means that the length of BC, in Fig. 6(a), is equal to the length of CB'. Note that the isotropic hardening rule is excluded from Bauschinger effect. Thus, the isotropic hardening rule can be expressed as

$$\sigma_{B'} = -\sigma_B \tag{4}$$

2. *Kinematic hardening rule*: The kinematic hardening rule by referring Fig. 6(b) is expressed as

$$\sigma_{B'} = \sigma_B - 2\sigma_y \tag{5}$$

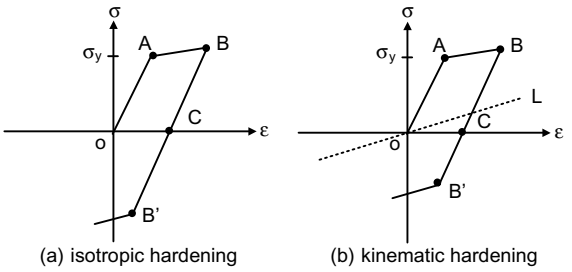

Fig. 6. The hardening rule of material.

Suppose the magnitude of elastic region $(\sigma_B - \sigma'_B)$ is constant, the center of elastic region moves along the straight line L and describes the Bauschinger effect.

3. *Hybrid-hardening rule*: Two surfaces theories of plasticity for explaining the effect of yield surface and boundary surface are applied on this mechanics behavior by simultaneously considering the isotropic hardening and kinematic hardening rules. In general, the nonlinear behavior is simulated by both surfaces with the hybrid-hardening rule—the yield surface or elastic part follows the kinematic hardening rule while the boundary surface obeys the isotropic hardening rule.

As shown on Fig. 7, the hysteresis loop of LYS-ADAS by Wen's model does not completely fit that by experimental results because of the lack of the isotropic hardening rule. Thus, the modified Wen's model by hybrid-hardening rule should be available to simulate practical mechanics behavior of LYS-ADAS.

2.3. Modified Wen's Model

In order to accurately depict the nonlinear behavior of LYS-ADAS under practical reciprocating loading, it is necessary to involve isotropic hardening within the Wen's Model. According to the envelope curve of maximum incremental displacement in each cycle of reciprocating loading test, it reveals that the hardening of boundary surface of LYS-ADAS approaches bi-linear transformation, shown in Fig. 8. Thus, the transformation of isotropic hardening of LYS-ADAS can be defined as

$$\Delta_y = \begin{cases} \Delta_{y0} & \text{if } \Delta_{\max} \leqslant \Delta_{y0} \\ \Delta_{y0} + \mu(\Delta_{\max} - \Delta_{y0}) & \text{if } \Delta_{\max} \geqslant \Delta_{y0} \end{cases} \tag{6}$$

where Δ_{y0} is the initial yielding displacement; $\Delta_{\max}$, absolute value of the maximum displacement in the

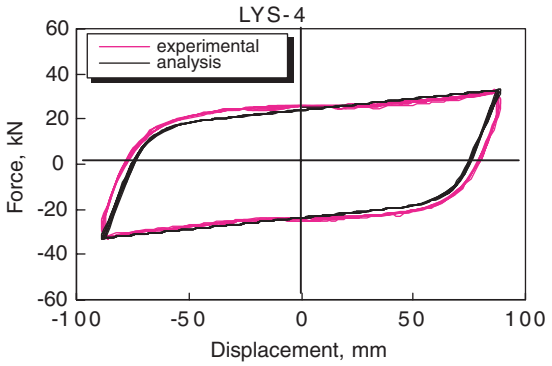

Fig. 7. The comparison of experimental and analysis method of Wen's model.

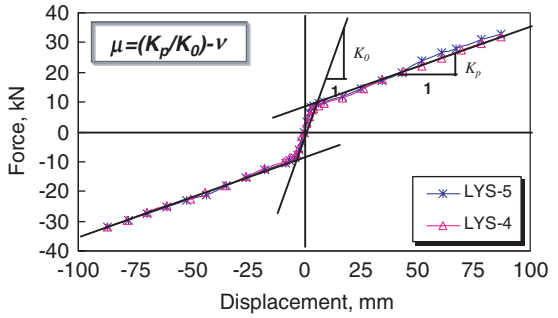

Fig. 8. The hardening behavior of envelope curve of LYS-ADAS.

loading history; μ, the difference between the ratio for the slope of second section to that of first section in the bi-linear function defined in this paper and the rate of kinematic transformation υ.

From Sues et al. [10], α is used to determine elastic stiffness of forced member; the yielding displacement, or the radius of yielding surface, is carried by the ratio of α to $\beta + \alpha$, i.e.,

$$K_e = K_0 \cdot \alpha \tag{7}$$

$$\Delta_y = \left(\frac{\alpha}{\beta+\gamma}\right)^{1/n} \tag{8}$$

where K_e, the initial stiffness, acquired by Wen's Model.

The experimental data shows that the elastic stiffness of ADAS almost remains the specified value and implies that α should be a constant as deforming. Furthermore, Fig. 8 indicates that the yielding displacement Δ_y increases corresponding to the maximum displacement. Therefore, the summation of β and γ should be decreased while the maximum displacement increases. Moreover, the new parameter is defined as the multiplier of β and γ. Thus, Eq. (2) can be modified as

$$\dot{q} = \alpha\dot{x} - \eta(\beta|\dot{x}||q|^{n-1}q + \gamma\dot{x}|q|^n) \tag{9}$$

$$\eta = \left(\frac{\Delta_y}{\Delta_{y0}}\right)^{-n} \tag{10}$$

where Δ_y, the present yielding displacement of ADAS, shown in Eq. (6); Δ_{y0}, the initial yielding displacement. η ranges from 0 to 1 and follows the transformation of deformation history, which is decreasing.

3. Parameters identification

If the transformed displacement variable q in Eq. (9) is differentiated by x, instead of time t, then it can be written as

$$q' = \frac{dq}{dx} = \alpha - \eta(\beta \cdot \mathrm{sign}(\dot{x})|q|^{n-1}q + \gamma|q|^n) \tag{11}$$

The discretization of Eq. (9) is

$$\Delta q_i = [\alpha - \eta_i(\beta \cdot \mathrm{sign}(\dot{x}_i)|q_i|^{n-1}q_i + \gamma|q_i|^n)]\Delta x_i \tag{12}$$

define

$$y_{1i} = \Delta x_i \tag{13a}$$

$$y_{2i} = (\eta_i \cdot \mathrm{sign}(\dot{x}_i)|q_i|^{n-1}q_i)\Delta x_i \tag{13b}$$

$$y_{3i} = (\eta_i|q_i|^n)\Delta x_i \tag{13c}$$

Then, Eq. (12) can be rewritten as

$$\Delta q_i = \alpha y_{1i} - \beta y_{2i} - \gamma y_{3i} \tag{14}$$

Thus, Δq_i is a linear function of y_{1i}, y_{2i}, y_{3i} as well as the optimal coefficients, α, β and γ, can be obtained by least square method. The method is described as follows: In Eq. (13), the displacement increment Δx_i are required from the test. Substitute restoring force R_i into Eq. (1) to determine q_i in this step

$$q_i = \frac{R_i - \upsilon K_0 x_i}{(1-\upsilon)K_0} \tag{15}$$

K_0 and υ can be estimated from the experimental data, and converged to a very good result after several iterations. The given hardening coefficient μ is substituted into x_i. Use Eq. (6) to judge the value of yielding displacement of Δ_{yi} at that step and substitutes it into Eq. (10) to acquire η_i of Eqs. (13b) and (13c).

Furthermore, x_i, q_i, and η_i can be substituted into Eqs. (13a–c) to obtain y_{1i}, y_{2i}, y_{3i} at each step. By least square method, q_0 should be set as zero, then the following simultaneous equations can be solved:

$$\begin{bmatrix} \sum y_{1i}^2 & -\sum y_{1i}y_{2i} & -\sum y_{1i}y_{3i} \\ & \sum y_{2i}^2 & \sum y_{2i}y_{3i} \\ \text{sym.} & & \sum y_{3i}^2 \end{bmatrix} \begin{Bmatrix} \alpha \\ \beta \\ \gamma \end{Bmatrix} = \begin{Bmatrix} \sum y_{1i}\Delta q_i \\ -\sum y_{2i}\Delta q_i \\ -\sum y_{3i}\Delta q_i \end{Bmatrix} \tag{16}$$

The above procedure can be seen in Fig. 9.

4. The optimal parameters of seismic resistance

A whole procedure of modified Wen's Model is proposed to analyze the LYS-ADAS. The displacement increasing under reciprocating loading test is fitted by the proposed identification technique. The method of statistic is used to acquire the optimal parameters. The error square root of fitting is used for fixed quantity, and the standard deviation is used for each test results to judge whether the modified model is suitable. These optimal parameters of members are applied to process two pseudo-dynamic tests. The accuracy of this new model can be investigated by any loading history. Nine reciprocating loading tests and five arbitrary loading

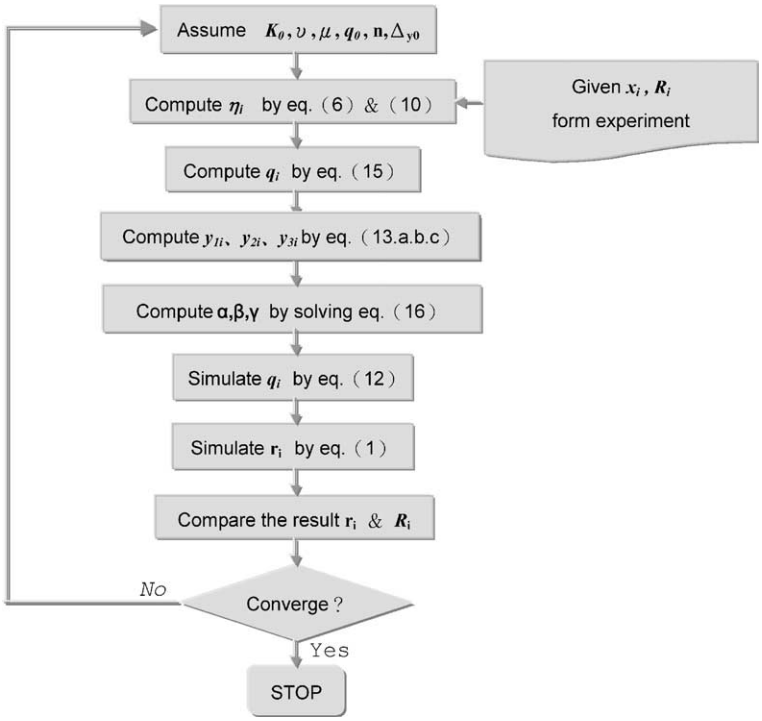

Fig. 9. The procedure of parameters identification of modified model.

tests executed in this investigation. All experiments are listed in Table 1.

The curves shown in Figs. 10–13 are obtained by substituting these optimal parameters into modified Wen's Model. These figures illustrate the simulation results of the experimental, optimal curve fitting and the proposed rules to determinate the parameters. Figs 10–13 show that the discrepancy between the proposed rule and the optimal parameters are quite rare. The suitability of this proposed method could be proved. All parameters identified from tests are listed in Table 2. The error, in Table 2, is defined as the ratio of average square root of difference, which occurs between test restoring and fitting force, to average square root of test restoring force. According to the identified results, the hardening behavior of ADAS can be concluded as follows:

Table 1
The experimental conditions of investigation

Specimen ID	Material	Loading type	Thickness (mm)	Height (mm)	K_0 (kN/mm)	Δ_{y0} (mm)
LYS-1	LYS100	Flexural	16	270	2.26	4.59
LYS-2	LYS100	Flexural	16	270	1.83	5.05
LYS-3	LYS100	Flexural	16	270	1.57	6.30
LYS-4	LYS100	Flexural	16	270	2.26	4.22
LYS-5	LYS100	Flexural	16	270	2.49	3.60
LB2-1	LYS100	Flexural	34.9	285	17.9	3.24
LA2-1	LYS235	Flexural	35.7	285	22.6	6.01
A36-1	A36	Flexural	16	270	2.604	11.9
A36R2-2	A36	Flexural	25	325	7.73	11.3
LYS-Kobe230g	LYS100	Flexural	16	270	1.80	5.1
A36-Kobe230g	A36	Flexural	16	270	2.43	12.75
LYP100-1	LYS100	Axial	NA	NA	1.85	0.041
LYP235-6	LYS235	Axial	NA	NA	1.89	0.109
A36-2 (R1)	A36	Axial	NA	NA	1.98	0.129

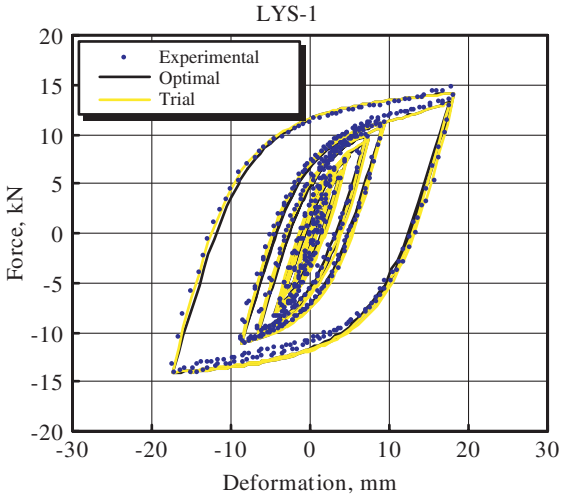

Fig. 10. The simulated results of LYS-1.

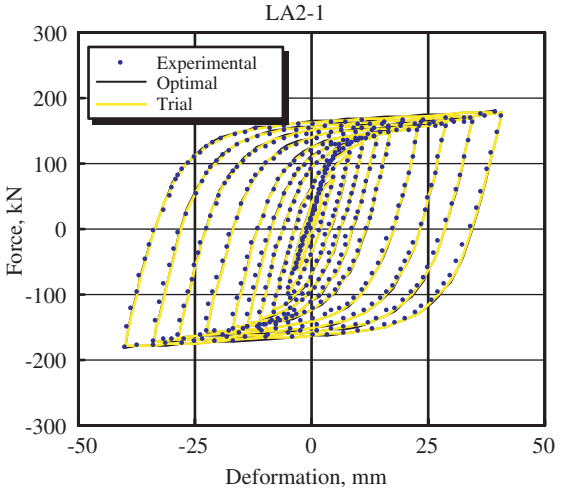

Fig. 12. The simulated results of LA2-1.

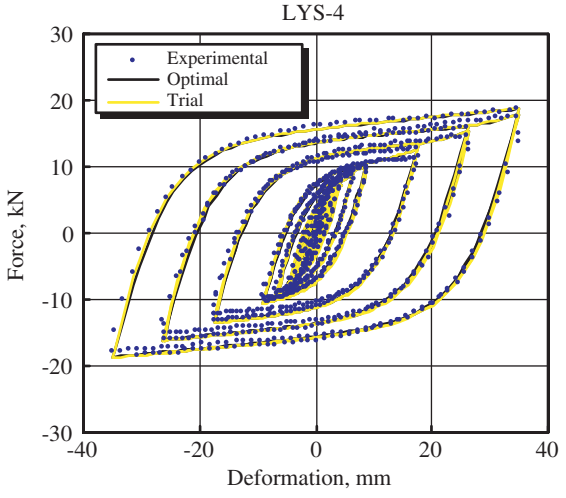

Fig. 11. The simulated results of LYS-4.

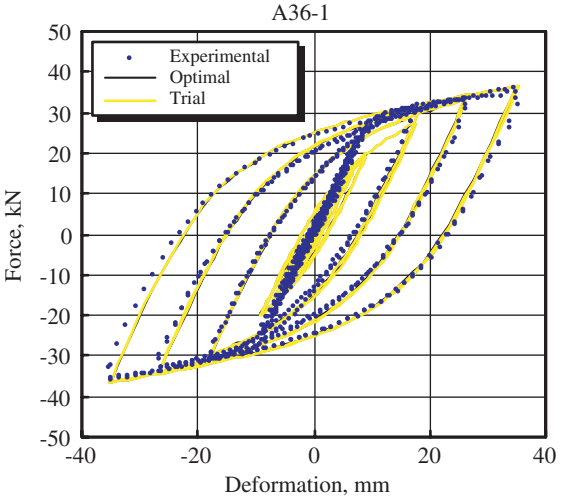

Fig. 13. The simulated results of A36-1.

1. *LYS100-ADAS*: the isotropic hardening coefficient μ is about three times of kinematic hardening coefficient υ for LYS100 steel. The sum of both coefficients is equal to the ratio of yielding stiffness K_p to initial stiffness K_0. The definition of LYS100 is the yielding stress = 100 MPA.
2. *LYS235-ADAS*: the isotropic hardening coefficient μ and kinematic hardening coefficient υ are almost the same as LYS235. The definition of LYS235 is the yielding stress = 235 MPA.
3. *A36-ADAS*: when the isotropic hardening coefficient μ is set as 0, the fitting is very well. In the other word, original Wen's Model works for it.

Additionally, in order to understand the influence of the ratio (β/γ), Eq. (8) can be used to acquire the sum of β and γ by the optimal K_0, Δ_{y0}, μ and υ, obtained from the identified results of known displacement history. The ratio (β/γ) should be adjusted in accordance with these values. The results show that the ratio (β/γ) has no influence in the simulated hysteresis loop. No matter how the steel is used, the ratio (β/γ) should be larger than 1.0. The numerical results suggest that the ratio (β/γ) must be greater than 3.0 for LYS100 and 1.0 for A36. From the discussions of fitting results, a whole set of parameters can be summed up. The flowchart to determine parameters is shown in Fig. 14.

To explore the effect of modified Wen's Model under any loading test, the pseudo-dynamic tests are executed for LYS100-ADAS and A36-ADAS. The initial stiffness and yielding displacement of test material are set as 1.803 kN/mm^2 and 5.1 mm, respectively. The final ratio

Table 2
The identified parameters results of each test

Specimen	K_p/K_0	Δ_{y0}	μ	υ	Regression by Eq. (16)				Trial (follow flow chart Fig. 14)			
					α	β	γ	Error	α	β	γ	Error
LYS-1	0.133	4.6	0.101	0.032	1.006	0.134	0.084	0.10	1.000	0.163	0.054	0.01
LYS-2	0.133	5.13	0.102	0.031	1.002	0.173	0.022	0.08	1.000	0.146	0.015	0.09
LYS-3	0.131	6.3	0.101	0.03	1.002	0.179	−0.020	0.08	1.000	0.136	0.023	0.10
LYS-4	0.131	4.39	0.1	0.031	1.001	0.176	0.052	0.06	1.000	0.182	0.046	0.07
LYS-5	0.133	3.6	0.101	0.032	1.001	0.223	0.054	0.06	1.000	0.222	0.056	0.07
LB2-1	0.128	3.17	0.096	0.032	1.002	0.410	−0.095	0.11	1.000	0.276	0.039	0.11
LA2-1	0.06	5.93	0.031	0.029	1.002	0.128	0.041	0.07	1.000	0.125	0.042	0.08
A36-1	0.095	11.886	0	0.095	1.001	0.054	0.030	0.12	1.000	0.056	0.028	0.12
A36R2-2	0.09	11.3	0	0.09	1.002	0.065	0.024	0.10	1.000	0.066	0.022	0.10

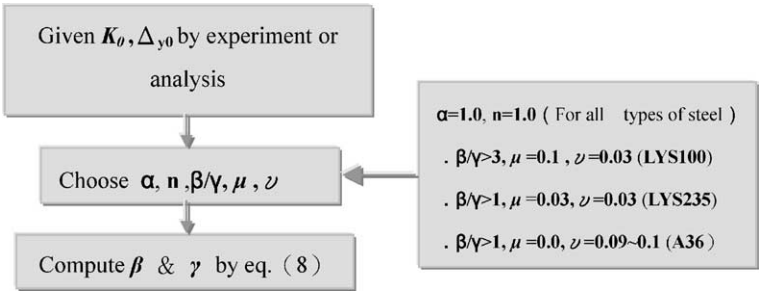

Fig. 14. The flowchart of setting parameters of modified Wen's model.

of yielding stiffness K_p to initial stiffness K_0 is 0.131. The other parameters listed in Table 2 follow the procedure shown in Fig. 14. The parameters set for LYS100 and A36 follow the same steps. The data of ground displacement of Kobe earthquake in 1995 are used to test both types of material. The results are shown in Fig. 15. We can observe that the tendency of hysteresis loops of simulated and test steel plate are almost merging together under arbitrary loading test by means of the identified parameters. Especially, the comparison of experimental and simulation results of LYS100-Kobe230g under the real ground motion record are matched very close. It indicates that the proposed model is pretty well in simulating the energy dissipation behavior of LYS-ADAS. Additionally, in order to investigate the simulated situation of various loading style of members, three other test results under the axial forces are selected to simulate and analyze. The modified Wen's Model predicts the displacement history of test. The parameters used in this simulation are listed in Table 2. The added displacement history and numerical results are shown in Fig. 16. The figures show that the modified Wen's Model also succeeds in predicting the axial force style of seismic resistance. The error of regression by Eq. (16) and the flow of parameters defined in Fig. 14 are below 12% and 11%, respectively, under these nine reciprocating loading tests.

5. Dynamic analysis

The total hardening rate of ADAS is determined by monotonic loading test, then, the kinematic hardening rate and isotropic hardening rate can be assigned by the ratio suggested in previous section. To estimate the loading on the damper for dynamical analysis, Eq. (9) must be discretized as the incremental function of transformed displacement q in Eq. (12). By Eq. (12), the increment of transformed displacement, Δq, is carried out with known displacement increment Δx. Once Δq is obtained, the total transformed displacement can be computed and substituted Eq. (1) into Eq. (12) for calculating member force.

Herein, the fourth-order Runge–Kutta differentiation algorithm is processed with state space formulation for seismic duration analysis or seismic history analysis. It requires four times of calculation of first-order differentiation of the state vector at different instants within a time step. For the case in this paper, the velocity and acceleration of lump mass is solved four times. The velocity can be directly acquired by state variables while the acceleration requests the total member force of mass components divided by mass. However, it is only the transit response during a time step and not sufficient to revise the hardening multiplier of Wen's module. Therefore, the proposed research suggests that the

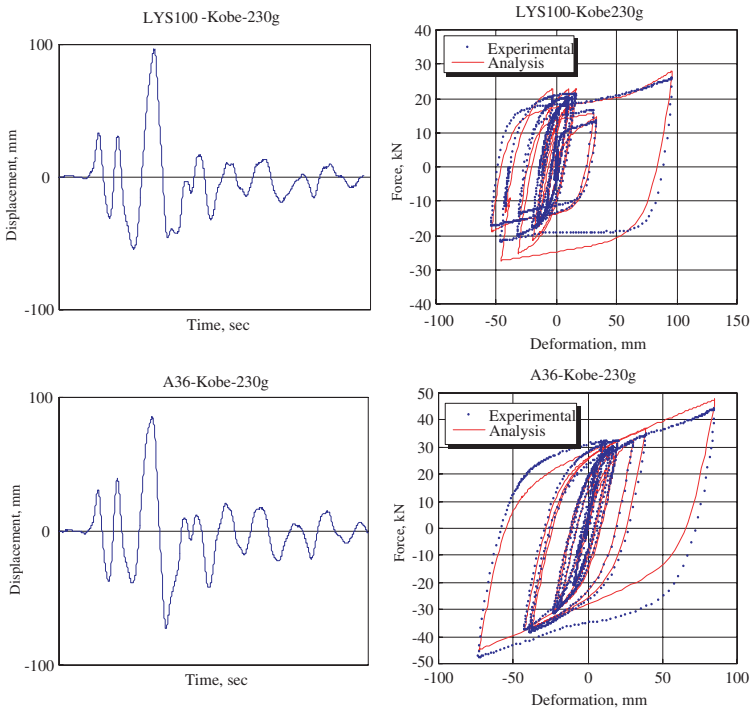

Fig. 15. The comparison of experimental and numerical results of LYS100 and A36 under ground motion record of Kobe, Japan 1994.

hardening multiplier should be constant as initial and be modified by Eq. (10) after finishing calculation of one time step. The detailed procedure is shown in Fig. 17.

5.1. Parameters for numerical analysis

To perform the adventure of modified Wen's module in analysis, the proposed research simulates the one-degree-of-freedom structure under earthquake history. The parameters of structure are established as follows:

Mass = 208.385 ton

Stiffness = 1049 kN/m

Damping coefficient = 9.352 kN s/m

The structure has natural period in 2.8 s, which is quite soft, so that ADAS is implemented to reduce displacement. Applied excitation is the acceleration of ground motion recorded by Japan Nokia earthquake, occurred in 1995, shown in Fig. 18. Four ADAS parameters shown in Table 3 are selected to precisely evaluate the effects of kinematic and isotropic hardening modules on the response of structure displacement. In which the first two sets of parameters ($S1$, $S2$) represent the ADAS with A36 steel.

In Table 1, the initial stiffness and yielding deflection of KADAS made of A36 steel, specimen A36-Kobe230g, are 2.43 kN/mm and 12.75 mm, respectively. From Table 2, the ADAS with A36 steel presents hardening rate approximately at 0.095, i.e., the slope of displacement–force relationship after yielding is about 9.5% of that before yielding. It implies that A36 steel has obscure isotropic hardening behavior since $S1$ performs kinematic hardening rate as 9.5% but zero isotropic hardening rate. $S2$, comparing with $S1$, follows the characteristics studied from LYS100 steel and adjusts the isotropic hardening rate as three times than kinematic hardening rate.

Furthermore, the parameter sets $S3$ and $S4$ represent the ADAS made of LYS100. With assistance of Tables 1 and 2, specimen LYS-Kobe230g, the initial stiffness, yielding deflection, and total hardening rate are 1.8 kN/mm, 5.1 mm, and 0.131, respectively. $S4$ is the optimal estimation based on the study of LYS and the ratio of isotropic and kinematic hardening rates (0.1 and 0.031, respectively) is about 3:1. $S3$, comparing with $S4$, setups 0 for isotopic hardening rate and 0.151 for kinematic hardening rate, the result will not be expected as correct as $S4$.

The dynamic analysis program GENDYN, which solves nonlinear kinematical equilibrium equations by the fourth-order Runge–Kutta method, works here for simulating these four damping systems. The flowchart in Fig. 17 demonstrates the algorithm of program for calculating member force of ADAS during each time

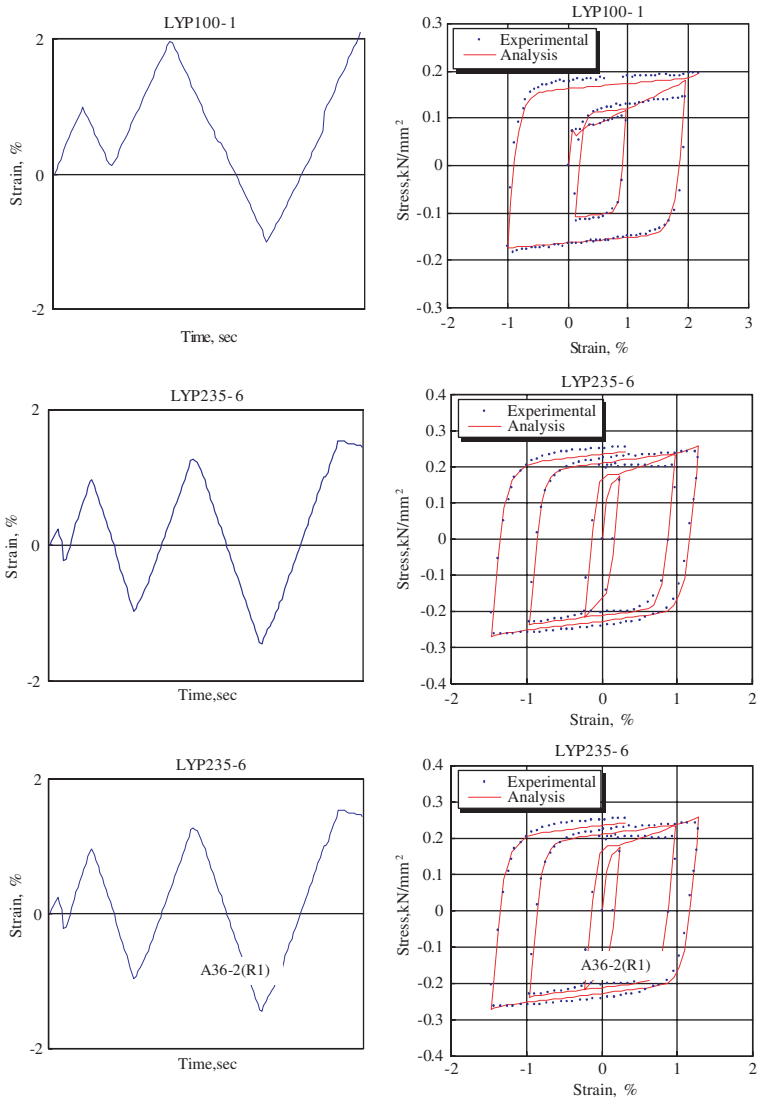

Fig. 16. The comparison of experimental and numerical results of added displacement history.

step and updating it for deformation after the step. For this case, the time step is 0.01 s.

Finally, the pseudo-dynamic test [15] is processed for A36 and LYS100 modules in the analysis to verify the result. Herein, this test is only applied on dampers as sub-structure test while the restoring and damping forces of structure are analyzed with numerical simulation.

6. The comparison of numerical analysis results

Fig. 19 presents simulation results and displacement history of the structure for the pseudo-dynamic test. Fig. 20 illustrates the relationship of damping force and displacement. Table 4 lists maximum displacement and square root of displacement for whole test and analysis. Fig. 20(a) indicates that modules with kinematic hardening analysis, or both of kinematic and isotropic hardening analyses, are able to properly simulate deformation–force relationship of A36 steel ADAS. However, the displacement history in Fig. 19(a) explains that hardening consideration has no significant effect on A36 steel ADAS.

With isotropic hardening characteristics, LYS100 performs large difference in the analysis with respect to A36 steel. In Fig. 19(b), if LYS100-ADAS simulation considers kinematic hardening only, it loses about 60% of energy dissipation capability with respect to that also involves isotropic hardening, and causes improper story

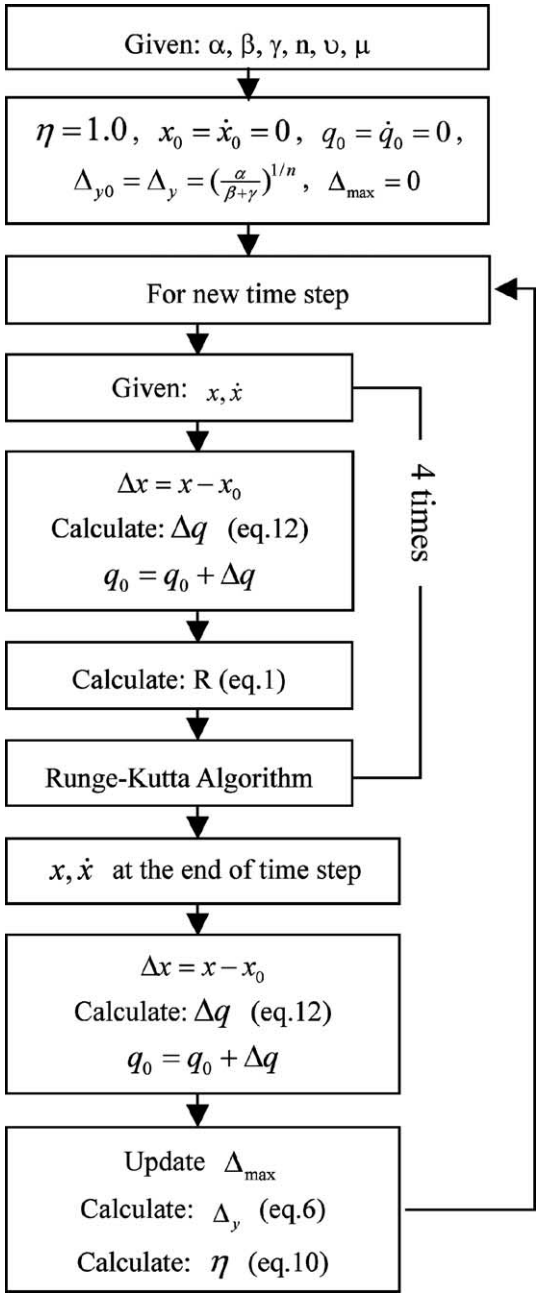

Fig. 17. Analysis flow chart.

drift. In the other word, the simulation results with both considerations of kinematic and isotropic hardening, instead of kinematic hardening only, is perfectly fitting experimental data.

The bi-linear module simulation is used to analyze elastoplastic behavior of A36 steel. The structural analysis is reliable though slight error might be counted. In this paper, the error is controlled within 1.04% and mean-value of square root of displacement is 3.18%. However, it is not suitable for LYS100 since the error approaches 7.70% while the mean-value of square root of displacement is 17.70%. If the consideration of isotropic hardening is involved, the error and mean-value of square root are eliminated to 0.95% and 0.37%, respectively.

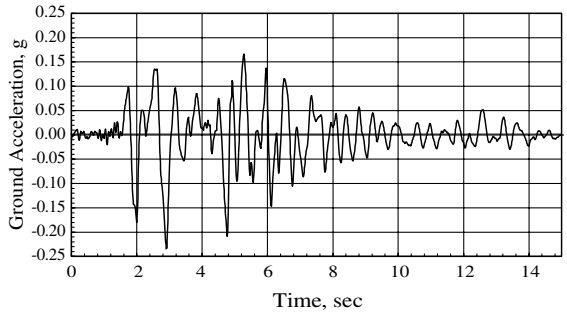

Fig. 18. Kobe earthquake, PGA scaled down to 0.23 g.

7. Discussion and conclusions

The test results of LYS-ADAS show that the bi-linear model for A36-ADAS cannot predict the behavior of LYS-ADAS effectively. The yielding displacements of LYS steel plate increases with the maximum displacement under the displacement increasing reciprocating loading test. The energy dissipation action of this proposed device indicates the transformed bi-linear behavior. Consequently, the hardening function of bi-linear and parameter η are defined to adjust the yielding displacement of modified Wen's Model that depends on displacement history. The following specific conclusions can be acquired in this research:

1. In order to perform the actual dissipation behavior of LYS100 steel plate, the isotropic hardening mechanism is added to modify the Wen's Model. Then, we can use the parameters identification from the modified model to predict the energy dissipation of LYS100 steel plate successfully.
2. Both of the experimental data and numerical results indicate that μ and υ are 0.1 and 0.03 for LYS100 steel plate, respectively.
3. μ is defined as 0 and υ ranges from 0.09 to 0.1 for A36-ADAS. For LYS235 steel plate, μ and υ should be equivalent, about 0.03.
4. To change the ratio (β/γ), it does not influence the simulated hysteresis loop greatly from the actual simulated results under the displacement increasing

Table 3
Analysis parameters

Data set	KADAS material	KADAS stiffness (kN/m)	μ	υ	α	β	γ	Δ_{y0} (m)
*S*1	A36	2430	0	0.095	1	52	26	0.01275
*S*2	A36	2430	0.071	0.024	1	52	26	0.01275
*S*3	LYS100	1800	0	0.1031	1	157	40	0.0051
*S*4	LYS100	1800	0.1	0.031	1	157	40	0.0051

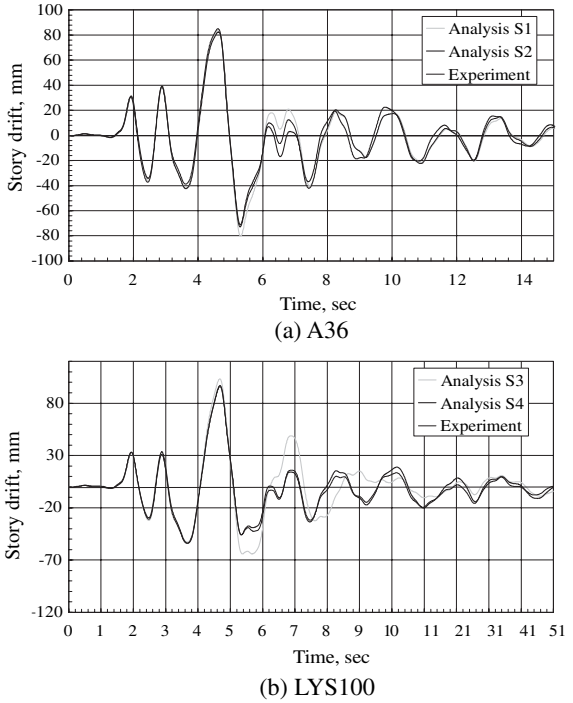

Fig. 19. Comparison of the story drift of analytical and pseudo-dynamic test results.

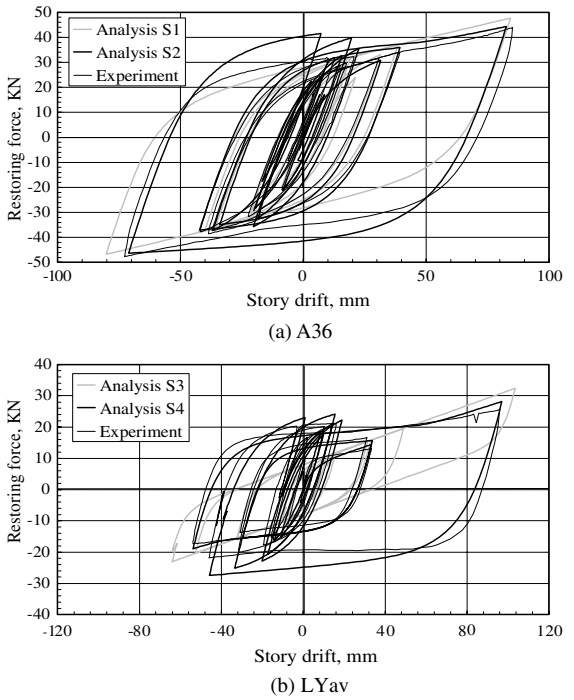

Fig. 20. Comparison of the restoring force of analytical and pseudo-dynamic test results.

reciprocating loading test. However, the ratio (β/γ) for LYS100 and A36 steel plate should be greater than 3.0 and 1.0, respectively.

5. As considering LYS as material of ADAS, both of kinematic and isotropic hardening behavior must be counted. The regular bi-linear model for this case will over estimate the maximum displacement.

The seismic dissipation capability of LYS material for metallic damper is superior to regular used material A36. Therefore, the Wen's model should be modified to predict the special mechanics behavior of LYS. From the test results show that the hysteresis energy dissipation performance of LYS-ADAS can be easily reflected under any loading test based on identified results to simulate the actual behavior of LYS-ADAS under the excitation of earthquake. The modified Wen's Model is a successful tool for the analysis of LYS-ADAS.

Table 4
Comparison of peak and RMS of story drift

Material	Data set	Displacement		RMS displacement	
		Value (mm)	Error (%)	Value (mm)	Error (%)
A36	Experiment	85.16	–	24.84	–
	*S*1	84.28	1.05	25.60	3.08
	*S*2	82.61	3.09	24.20	2.49
LYS100	Experiment	96.08	–	24.15	–
	*S*3	103.47	7.15	28.30	14.61
	*S*4	96.99	0.95	34.20	0.37

Acknowledgments

This work has been supported by the National Science Council of Taiwan, ROC through grant no. NSC-93-2625-Z-327-003 and China Steel Corporation Company. These supports are gratefully acknowledged. The authors would also like to thank anonymous referees for their careful reading of the paper and several suggestions, which have helped to improve the paper.

References

[1] Tsai CS, Le HH. Applications of viscoelastic dampers to high-rise buildings. J Struct Eng, ASCE 1993;119(4): 1222–33.
[2] Tsai CS, Tsai KC. TPEA device as seismic damper for high rise buildings. J Eng Mech 1995;121(10):1075–81.
[3] Tsai KC, Chen HW, Hong CP, Su YF. Design of steel triangular plate energy absorbers for earthquake resistant construction. Earthquake Spectra 1993;9(3):517–50.
[4] Tsai KC, Chou CC. Plasticity models and seismic performance of steel plate energy dissipaters. J Chin Inst Civil Hydr Eng 1996;8(1):45–54.
[5] Sozen MA. Hysteresis in structural elements. In: Iwan WD, editor. Appl Mech Earthquake Eng. ASME; 1974. p. 63–98.
[6] Chang JT, Wang SC. The development of ultra low yield strength plate shell. China Steel Technical Report, No. 11; 1997.
[7] Sung WP, Shih MH, Chen KS. Analytical method for promoting process capability of shock absorption steel. J Zhejiang Univ Sci 2003;4(4):388–92.
[8] Tsai KC, Chou CC. Plastic fiber models of triangular plate energy dissipation device. Earthquake Eng Struct Dyn 2002;31:1643–55.
[9] Wen YK. Method for random vibration of hysteretic system. J Eng Mech, ASCE 1976;102(2):249–63.
[10] Sues RH, Mau ST, Wen YK. System identification of degrading hysteretic restoring forces. J Eng Mech 1988; 114(5):833–46.
[11] Bouc R. Forced vibration of mechanical system with hysteresis. In: Proceedings of the 4th International Conference on Nonlinear Oscillations, Prague, Czechoslovakia, 1967.
[12] Foliente GC. Hysteretic modeling of wood joints and structural systems. J Struct Eng, ASCE 1995;121(7): 1013–22.
[13] Barber T, Wen Y. Seismic response of hysteretic degrading structures. Publ Turk Natl Comm on Earthquake Eng 1980;7:457–64.
[14] Zhang H, Paevere P, Yang Y, Foliente GC, Ma F. System identification of hysteretic structures. In: IUTAM Symposium on Nonlinearity and Stochastic Structural Dynamics, 2001. p. 289–306.
[15] Mahin SA, Shing PB. Pseudodynamic method for seismic testing. J Struct Eng 1985;111(7):1482–585.